Korean J. Chem. Eng., 36(9), 1466-1473 (2019)
DOI: 10.1007/s11814-019-0333-8

pISSN: 0256-1115
eISSN: 1975-7220

Monoolein cubosomes for enhancement of *in vitro* anti-oxidative efficacy of Bambusae Caulis in Taeniam extract toward carcinogenic fine dust-stimulated RAW 264.7 cells

Seok Ho Park and Jin-Chul Kim†

Department of Medical Biomaterials Engineering, College of Biomedical Science and Institute of Bioscience and Biotechnology, Kangwon National University, 192-1, Hyoja 2 dong, Chunchon, Kangwon-do 24341, Korea
(*Received 14 February 2019 • accepted July 3, 2019*)

Abstract−Monoolein cubosomes was prepared for enhancement of *in vitro* anti-oxidative efficacy of Bambusae Caulis in Taeniam extract (BCT) toward carcinogenic fine dust-stimulated RAW 264.7 cells. Hydrophobicized alginate (HpAlg) and gelatin (HpGel) were included as potential actuators for controlled release. The loading of additives (i.e., BCT, HpAlg, and HpGel) led to a decrease in the phase transition temperature of the cubic phase, evidenced by polarized optical microscopy. The hydrodynamic diameter of cubosomes was 148 to 187 nm, and it seemed not to be affected by the additives. Cubosome promoted the *in vitro* skin permeation of BCT more effectively than hydroxypropyl-β-cyclodextrin, a skin permeation enhancer. Cubosomal BCT was more efficacious than free BCT in scavenging 2,2-diphenyl-1-picrylhydrazyl free radical and the intracellular reactive oxygen species of RAW 264.7 cells stimulated by carcinogenic fine dust. The internalization of cubosomes into cells, confirmed by fluorescence-activated cell sorting and super sensitive high resolution confocal laser scanning microscopy, could account for the higher radical-scavenging efficacy.

Keywords: Extract of Bambusae Caulis in Taeniam, Cubic Phase, Carcinogenic Fine Dust, RAW 264.7 Cell, ROS-scavenging Efficacy, Cellular Internalization

INTRODUCTION

The monoolein (MO) cubic phase has been one of the attractive drug carriers owing to its various beneficial characteristics for drug delivery [1-6]. MO is an amphiphilic molecule that can be assembled into cubic phase when hydrated with a sufficient amount of aqueous phase [1,7-11]. A cube is the crystallographic unit of the cubic phase and it has intercrossing water channels (about 5 nm in diameter) surrounded by MO bilayers (about 3.5 nm in thickness). MO cubic phase can imbibe water as much as 28 to 40% (w/w, based on the weight of the cubic phase), and it can hardly be formed if the water content is less than the lower limit [1,12,13]. Both hydrophilic compounds and lipophilic ones can be loaded in the cubic phase because the water channel is the polar compartment and the lipid bilayer is the non-polar one. In this study, MO cubosome was prepared to promote the skin permeation of Bambusae Caulis in Taeniam extract (BCT) and enhance the *in vitro* anti-oxidative efficacy of BCT toward carcinogenic fine dust-stimulated RAW 264.7 cells. Hydrophobicized alginate (HpAlg) and gelatin (HpGel) were included in the cubosomes as potential actuators for controlled release. HpAlg is a negatively charged polysaccharide and HpGel is a amphoteric protein. Accordingly, HpAlg and HpGel can form a complex coacervate in the water channel of MO cubic phase in the present experimental pH condition (pH 4.5), and the coacervate is be able to hinder the diffusion of a diffusate [14]. The coacervate is capable of preventing a burst and fast release of the cubosomal payload before the cubosomes are internalized into cells [15]; thus it would help the cubosomes to exhibit a high anti-oxidation efficacy. The effect of cubosome on the skin permeation of BCT was investigated using an artificial skin-mounted diffusion cell. Particulate drug carriers can be taken up by the cells by phagocytosis [16-21]. Thus, the cubosome was thought to be internalized into the cells and enhanced the transport of its payload (BCT) to the cells, leading to an increase in the biological efficacy of BCT (Fig. 1). The cells were stimulated by a carcinogenic fine dust to cause an inflammatory response and to promote the intracellular reactive oxygen species (ROS) production. The anti-oxidative efficacy of cubosomal BCT and free BCT was examined by observing the 2,2-diphenyl-1-picrylhydrazyl radical-scavenging and the intracellular ROS-scavenging capability. The transport of fluorescent-labelled cubosomes into the cells was investigated by fluorescence-activated cell sorting and super sensitive high resolution confocal laser scanning microscopy using calcein as a fluorescent dye.

MATERIAL AND METHODS

1. Materials

Hydrophobicized alginate (HpAlg) and gelatin (HpGel) were those prepared in a previous work [22]. Bambusae Caulis in Taeniam (BCT) extract was provided by UAT (Gimpo, Korea). MO Monomuls 90-O18 (monoolein, MO) was donated by ATEC CO., LTD. (Daejeon, Korea). 4-Hydroxybenzaldehyde (HBA), 4′,6-diamid-

†To whom correspondence should be addressed.
E-mail: jinkim@kangwon.ac.kr

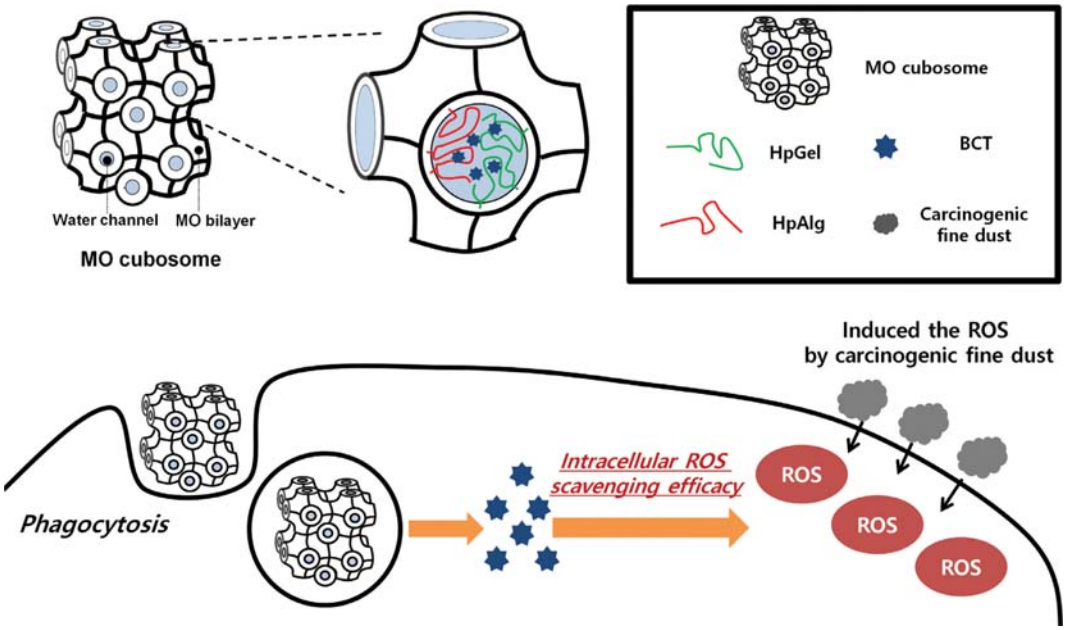

Fig. 1. Scheme of BCT loaded-cubosome (CS(BCT/HpAlg/HpGel)). The cubosome can be internalized into RAW 264.7 cells by phagocytosis and expedite the transfer of its cargo (i.e., BCT) to cells. As a result, the cubosome would be able to enhance the biological activity of BCT (i.e., efficacy in scavenging the intracellular ROS of the cells stimulated by carcinogenic fine dust).

ino-2-phenylindole (DAPI), calcein, Pluronic F127, (2-hydroxypropyl)-β-cyclodextrin (HP-β-CD), 2-(N-morpholino)ethanesulfonic acid (MES), sodium citrate, 2,2-diphenyl-1-picrylhydrazyl (DPPH), ascorbic acid, dichloro-dihydro-fluorescein diacetate (DCFH-DA), Hank's balanced salt solution (HBSS) were purchased from Sigma-Aldrich Co. (St. Louis, MO, USA). Acetonitrile (AN), acetic acid (AA) were purchased from Daejung Chemicals & Metals Co. (Siheung, Korea). Phosphate-buffered saline (PBS), trypsin/EDTA, Dulbecco's modification of Eagle medium (DMEM) were purchased from Thermo Fisher Scientific (Massachusetts, USA). Triton X-100, Trolox were purchased from Tokyo Chemical Industry Co., Ltd. (Tokyo, Japan).

2. Preparation of Cubic Phase

MO cubic phases were prepared by a melt hydration method [15,23,24]. BCT solution (4% (w/v), in sodium citrate buffer (10 mM, pH 4.5)) was used as an aqueous phase for the preparation of cubic phases. When required, HpAlg and/or HpGel were dissolved in BCT solution so that each concentration was 1% (w/v). 2 g of MO contained in a 20 ml vial was melted in a water bath (48-53 °C). 0.857 ml of BCT aqueous solution was warmed at the same temperature and slowly added over MO melt. The vial was tightly sealed and the aqueous solution/MO melt mixture stood at room temperature for ten days under dark condition for the formation of a homogeneous clear gel (i.e., cubic phase). Empty cubic phase, cubic phase containing BCT, BCT/HpAlg, BCT/HpGel, and BCT/HpAlg/HpGel were termed as CP(NO), CP(BCT), CP(BCT/HpAlg), CP(BCT/HpGel), and CP(BCT/HpAlg/HpGel), respectively. When the cubic phase was necessary to be fluorescently labelled for fluorescence-activated cell sorting (FACS) and super sensitive high resolution confocal laser scanning microscopy (SR-CLSM), calcein (a water-soluble fluorescence dye) was dissolved in the aqueous solution prepared for the hydration of MO melt so that the concentration was 60 mg/ml.

3. Observation of Phase Transition by Polarized Optical Microscopy

The phase transition temperature of cubic phases was observed by a method described elsewhere [25-27]. Each of cubic phases was put in a cell comprising two parallel cover glasses, spaced by an O ring (6 mm in inner diameter and 0.1 mm in thickness), and the cell was placed in a heating block (HS81, Mettler Toledo, USA). While being heated from 25-80 °C, the texture of each cubic phase was observed on a polarized optical microscope.

4. Preparation of Cubic Phase Nanoparticles

Cubic phase nanoparticles (cubosomes) were prepared via the micronization of cubic phase using a sonicator. 25 mg of cubic phase lump was put in 5 ml of Pluronic F127 solution (0.1% (w/v)) contained in a 10 ml glass vial then it was micronized for 1 hr on a tip type sonicator (VC 505, Sonic & Materials, USA, pulse on: 30 s, off: 40 s). Micronized cubic phases, cubosomes, were abbreviated to CS(NO), CS(BCT), CS(BCT/HpAlg), CS(BCT/HpGel), and CS (BCT/HpAlg/HpGel).

5. Measurement of Hydrodynamic Diameter of Cubosomes

Dynamic light scattering was employed to determine the hydrodynamic diameter of cubosomes. The light scattering intensity of cubosomal suspensions was made to be 200-400 Kcps by diluting the suspension with distilled water. The size distribution and the mean diameter were determined on light scattering equipment (Plus 90, Brookhaven Instrument, USA).

6. Evaluation of Skin Permeation of 4-HBA

Skin permeation of 4-HBA (a hydrophobic ingredient of BCT) was investigated using Franz diffusion cells (0.636 cm^2 surface area). An artificial skin (Strat-M® Membrane, EMD millipore corpora-

tion, USA) was mounted between the donor chamber and receptor one of the diffusion cell. The receptor chamber was filled with 5 ml of HP-β-CD solution (50 mg/ml, in MES buffer (10 mM, pH 5.5)), then 1.2 ml each of samples was applied on the skin exposed to the donor chamber. BCT solution (2.88 mg BCT/ml, in sodium citrate buffer (10 mM, pH 4.5)), BCT solution (2.88 mg BCT/ml, in HP-β-CD solution (50 mg/ml, in sodium citrate buffer (10 mM, pH 4.5))), and CS(BCT/HpAlg/HpGel) suspension (2.88 mg BCT/ml, in sodium citrate buffer (10 mM, pH 4.5)) were used as test samples. 100 μl was taken from the receptor chamber through a sampling port at a given time and assayed for 4-HBA by high performance liquid chromatography analysis. The amount of 4-HBA was determined using the peak area on elution profile and a calibration curve. A column (C18, 5 μm, 250×4.6 mm, Phenomenex) was eluted with AN/AA solution (1%, v/v) (1/9, v/v) flowing at rate of 0.8 ml/min, and 10 μl of the receptor solution was injected into the column. A gradient elution was applied to the column using AN/AA (2/8, v/v) in 0-15 min, AN/AA (4/6, v/v) in 15-40 min, and AN/AA (5/5, v/v) in 40-60 min. A diode-array detector could detect 4-HBA quantitatively at 330 nm [22,28,29].

7. DPPH Radical Scavenging Efficacy

BCT solution (in PBS (135 mM NaCl, 2.7 mM KCl, 4.3 mM Na_2HPO_4, 1.4 mM KH_2PO_4, pH 7.4)) and CS(BCT/HpAlg/HpGel) suspension (in PBS (135 mM NaCl, 2.7 mM KCl, 4.3 mM Na_2HPO_4, 1.4 mM KH_2PO_4, pH 7.4)) were used as test samples, ascorbic acid solution as a positive control, and blank distilled water as a negative control. DPPH was dissolved in ethanol so that the concentration was 0.2 mM. 100 μl of DPPH solution was mixed with the same amount of each of test samples and controls, and the mixture stood at 30 °C for 1 h under dark condition for the reduction of DPPH radical. The absorbance at 517 nm of each mixture was measured on a UV spectrophotometer (6505 UV/Vis. Spectrophotometer, JENWAY, UK). The wavelength of 517 nm is the characteristic wavelength of reduced form of DPPH. DPPH radical scavenging efficacy was calculated by an equation, RCE (%)=(1−Ab_s/Ab_c)×100, where RC (%) was DPPH radical scavenging efficacy in %, Ab_s was the absorbance of DPPH solution containing a test sample or a positive control, and Ab_c was the absorbance of DPPH solution containing a negative control [30-32].

8. Intracellular ROS Scavenging Efficacy

CS(BCT/HpAlg/HpGel) suspension was diluted with PBS (135 mM NaCl, 2.7 mM KCl, 4.3 mM Na_2HPO_4, 1.4 mM KH_2PO_4, pH 7.4) so that the concentration of BCT was 0.048, 0.24, 0.48, 0.98, and 1.92 μg/ml. Prepared was BCT solution (in PBS (135 mM NaCl, 2.7 mM KCl, 4.3 mM Na_2HPO_4, 1.4 mM KH_2PO_4, pH 7.4)) whose concentration was the same as that of the cubosomal suspension. RAW 264.7 cell (1×10^5 cells/mL, in FBS-free DMEM), 200 μl, was allocated to the each well of a 96-well plate, and cultured for 12 h in a CO_2 incubator (37 °C). Following culture medium (DMEM) was removed, 100 μl of the culture medium, 50 μl of a carcinogenic fine dust suspension (600 μg/ml), and 50 μl of a sample (a test sample: free BCT solution or CS(BCT/HpAlg/HpGel) suspension, a control: Trolox solution or PBS (135 mM NaCl, 2.7 mM KCl, 4.3 mM Na_2HPO_4, 1.4 mM KH_2PO_4, pH 7.4) was added to the each well and incubated for 24 h in a CO_2 incubator (37 °C). Trolox solution (250 μg/ml, in PBS (135 mM NaCl, 2.7 mM KCl, 4.3 mM Na_2HPO_4, 1.4 mM KH_2PO_4, pH 7.4)) and blank PBS (135 mM NaCl, 2.7 mM KCl, 4.3 mM Na_2HPO_4, 1.4 mM KH_2PO_4, pH 7.4) were used as a positive and a native control, respectively. In parallel, the cells were not treated with the fine dust, then they were compared with the cells treated with only the fine dust (a negative control) in terms of ROS production to confirm that the fine dust could stimulate RAW 264.7 cell to produce more ROS. After the DMEM was decanted, the cells were washed with HBSS. 100 μl of DCFH-DA solution (20 μM, in HBSS) was added to the each well and they were incubated at 37 °C for 30 min to dye intracellular ROS to be fluorescent. The supernatant was discarded, 100 μl of Triton X-100 solution (1% (v/v), in HBSS) was added to the each well, and they stood at 37 °C for 30 min. The fluorescence intensity of solution contained in the each well was measured at 504 nm on a fluorescence plate reader (Synergy H1, Biotek, USA) using the excitation wavelength of 529 nm. ROS scavenging efficacy (ROS SE) was calculated by an equation, ROS SE (%)=(1−F_s/F_c)×100, where F_s is the florescence intensity of cells treated with the fine dust plus a test sample or the fine dust plus a positive control, and F_c is the fluorescence intensity of cells treated with only fine dust (a negative control).

9. Cellular Uptake of Cubosomes

RAW 264.7 cell suspended in DMEM with FBS, 1 ml, was dispensed in a 12-well plate so that the each well contained 3×10^6 cells, then cultured for 12 h in a CO_2 incubator thermostated at 37 °C. Cells were cleaned by washing them with PBS (135 mM NaCl, 2.7 mM KCl, 4.3 mM Na_2HPO_4, 1.4 mM KH_2PO_4, pH 7.4) after removing the DMEM. 0.1 ml of DMEM free of FBS, together with the same amount of a test sample (cubosomal calcein suspension or free calcein solution), were put in the each well and they were incubated for 0-6 h for the interaction of the cells and the test samples. The cells were washed with the buffer solution to remove free and cubosomal calcein. The cells were detached from the well wall by trypsin/EDTA treatment and suspended in PBS (135 mM NaClf, 2.7 mM KCl, 4.3 mM Na_2HPO_4, 1.4 mM KH_2PO_4, pH 7.4, 4 °C). The fluorescence intensity of calcein was determined at 515 nm on a flow cytometer (FACS Calibur, Becton Dickinson, USA, in the Central Laboratory of Kangwon National University) using the excitation wave length of 495 nm. The interaction of free or cubosomal calcein with the cells was also investigated by SR-CLSM. The culture conditions for SR-CLSM were the same as those for the flow cytometry. After the cells were incubated with free or cubosomal calcein, they were treated with 200 μl of formaldehyde solution (2.5% (v/v)) for 30 min for the structural fixation. The cells were washed with the buffer solution and they were treated with DAPI to dye the nuclei. Free dye was removed by washing the dyed cells with the buffer solution and the fluorescence images were taken on a SR-CLSM (LSM880, Carl Zeiss, Germany, in the Central Laboratory of Kangwon National University).

RESULTS AND DISCUSSION

1. Observation of Phase Transition by Polarized Optical Microscopy

Fig. 2 shows the polarized optical micrographs of CP(NO), CP(BCT), CP(BCT/HpAlg), CP(BCT/HpGel), and CP(BCT/HpAlg/

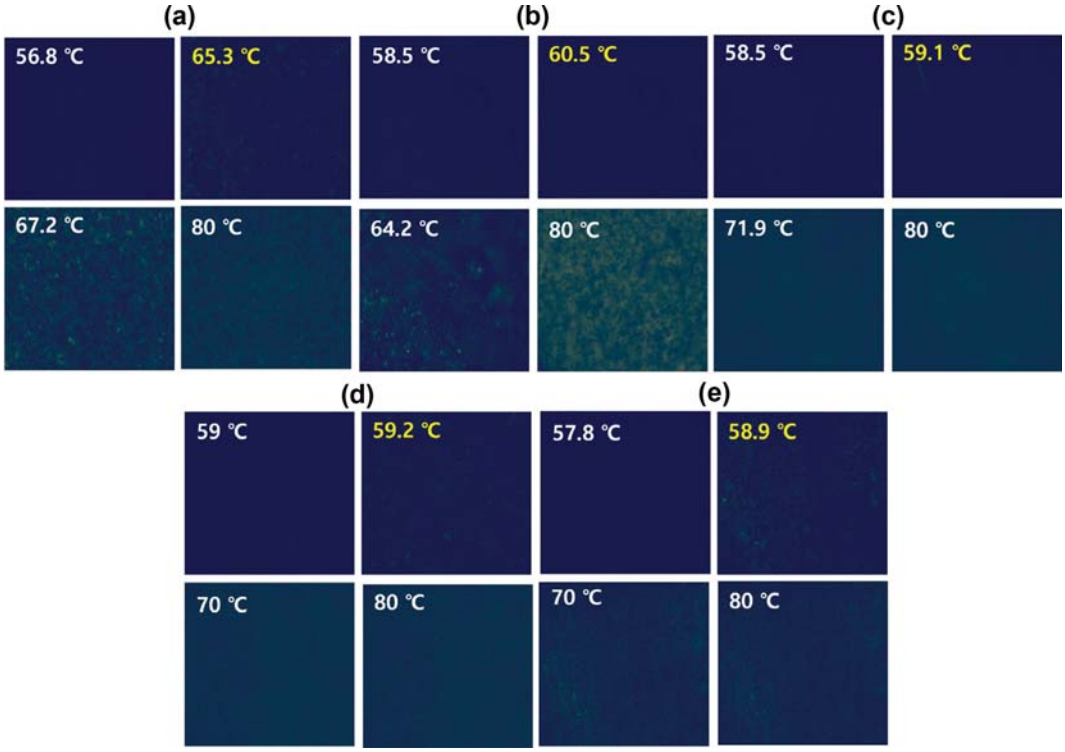

Fig. 2. Polarized optical micrographs of CP(NO) (a), CP(BCT) (b), CP(BCT/HpAlg) (c), CP(BCT/HpGel) (d), and CP(BCT/HpAlg/HpGel) (e).

HpGel). CP(NO) exhibited clean textures when the temperature was less than 65.3 °C, but showed birefringence when the temperature reached that temperature. The temperature where birefringence began to take place can be considered as a cubic-to-hexagonal phase transition because cubic phase is optically isotropic but hexagonal one is non-isotropic [26,33]. The phase transition temperature of CP(BCT) was about 60.5 °C, about 5 °C lower than that of CP(NO). An oil-soluble ingredient of BCT (e.g., 4-HBA) would be solubilized in the bilayer of cubic phase and increase its fluidity, leading to a decrease in the phase transition temperature. Inclusion of hydrophobicized polymers (HpAlg and HpGel) resulted in further decrease in the phase transition temperature. For example, the phase transition temperature of CP(BCT/HpAlg), CP(BCT/HpGel), and CP(BCT/HpAlg/HpGel) was 59.1 °C, 59.2 °C, and 58.9 °C, respectively, lower than that of CP(BCT). The hydrophobic anchor (decanoyl group) was thought to be incorporated into the bilayer and to fluidize it, giving a rise to decrease in the phase transition temperature.

2. Measurement of Hydrodynamic Diameter of Cubosomes

The size distribution of all the cubosomes prepare in present study was unimodal and narrow (distribution span was less than 200 nm, supplementary Fig. 1). Thus, it could be said that all the cubosomes were somewhat homogeneous in terms of size. The determinant factors affecting the size would be the concentration of dispersant (Pluronic F127), the MO/dispersant ratio, the micronization intensity, and the micronization duration. Since the cubosomes were small and homogeneous, the preparation conditions used in present study were thought to be worth being adopted in preparing MO cubosomes.

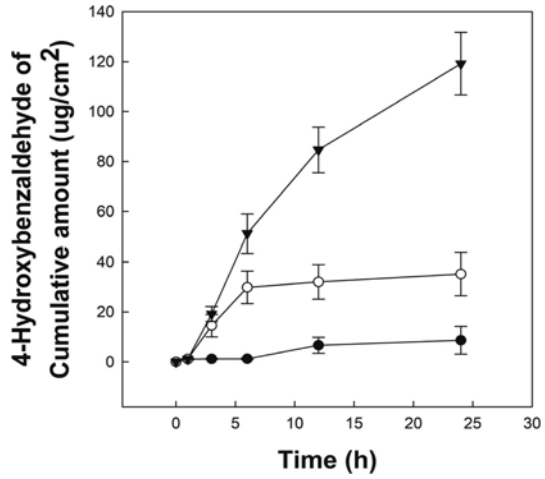

Fig. 3. Cumulative amount of 4-HBA permeated through a skin for 24 h when BCT solution (in sodium citrate buffer (10 mM, pH 4.5)) (●), BCT solution (in HP-β-CD solution (50 mg/ml, in sodium citrate buffer (10 mM, pH 4.5))) (○), and CS(BCT/HpAlg/HpGel) suspension (in sodium citrate buffer (10 mM, pH 4.5)) (▼) were applied on the skin.

3. Evaluation of Skin Permeation of 4-HBA

Fig. 3 shows the cumulative amount of 4-HBA permeated through a skin for 24 h when BCT solution (in sodium citrate buffer (10 mM, pH 4.5)), BCT solution (in HP-β-CD solution (50 mg/ml, in sodium citrate buffer (10 mM, pH 4.5))), and CS(BCT/HpAlg/HpGel) suspension (in sodium citrate buffer (10 mM, pH 4.5)) were applied on the skin. When BCT solution (in sodium citrate

buffer (10 mM, pH 4.5)) was used, the permeation amount did not appreciably increase for the first 6 h, then slightly increased to about 7 μg/cm^2 during the remaining period. When BCT solution (in HP-β-CD solution (50 mg/ml, in sodium citrate buffer (10 mM, pH 4.5))) was applied, the permeation amount markedly increased to 26 μg/cm^2 for the first 3 h, followed by a slow increase during the remaining period. HP-β-CD would hydrophobically interact with the lipidic components of skin owing to its hydrophobic cavity; thus it would be able to promote the skin permeation of 4-HBA. In fact, HP-β-CD is being used as a skin permeation enhancer [34-38]. When CS(BCT/HpAlg/HpGel) suspension was applied on skin, the permeation amount steadily increased to 120 μg/cm^2 during the whole period, and it was much more than the permeation amount obtained using BCT solutions. Cubosome has an affinity with skin because MO can hydrophobically interact with the lipidic components of skin [39-41]. In addition, cubosome is flexible and is able to penetrate into skin by adapting their shape to the tortuous transdermal pathway [42,43]. As a result, the skin permeation of a compound can be promoted, once it is loaded in MO cubosome.

4. DPPH Radical Scavenging Efficacy

Fig. 4(a) shows the DPPH radical-scavenging efficacy (RSE) of CS(BCT/HpAlg/HpGel). The RSE of ascorbic acid was about 56%. Ascorbic acid is vitamin C and it is well known to be an anti-oxidative agent [44-46]. CS(BCT/HpAlg/HpGel) exhibited a significant RSE at all the concentrations tested ($p<0.001$) and RSE was proportional to the concentration. For example, RSE was 32.5%, 37.9%, 41.2%, 45.1%, 49.2%, and 58.1%, respectively, when the concentration of BCT was 0.0024, 0.0048, 0.006, 0.012, 0.024, and 0.048 mg/ml. RSE obtained at the BCT concentration of 0.048 mg/ml was almost the same as RSE at the ascorbic concentration of 0.1 mg/ml. That is, even when the concentration of BCT was less than half of that of ascorbic acid, BCT loaded in cubosome (CS(BCT/HpAlg/HpGel)) seemed to be as potent as the vitamin in terms of scavenging DPPH free radical. Fig. 4(b) shows the RSE of free BCT. BCT also showed a significant RSE at all the concentrations tested ($p<0.001$) and RSE increased with increasing the concentration. For example, RSE was 25%, 30.8%, 34.8%, 38.7%, 42%, and 50.4%, respectively, when the concentration of BCT was 0.0024, 0.0048, 0.006, 0.012, 0.024, and 0.048 mg/ml. RSE obtained at the concentration of 0.048 mg/ml was about 90% of RSE at the ascorbic acid concentration of 0.1 mg/ml. That is, even when the concentration of BCT was less than half of that of ascorbic acid, the RSE of BCT was close to that of the vitamin. Thus, it could be said that BCT was efficacious in terms of scavenging DPPH free radical. The RSE of BCT loaded in CS(BCT/HpAlg/HpGel) was higher than that of free BCT at all concentrations tested (Fig. 4(a) and (b)). MO was the major component of the cubosome. Due to the double bond in its tail, it would be readily oxidized while reducing DPPH radical. This might account for why BCT loaded in CS (BCT/HpAlg/HpGel) exhibited higher RSE, but it was not clear yet.

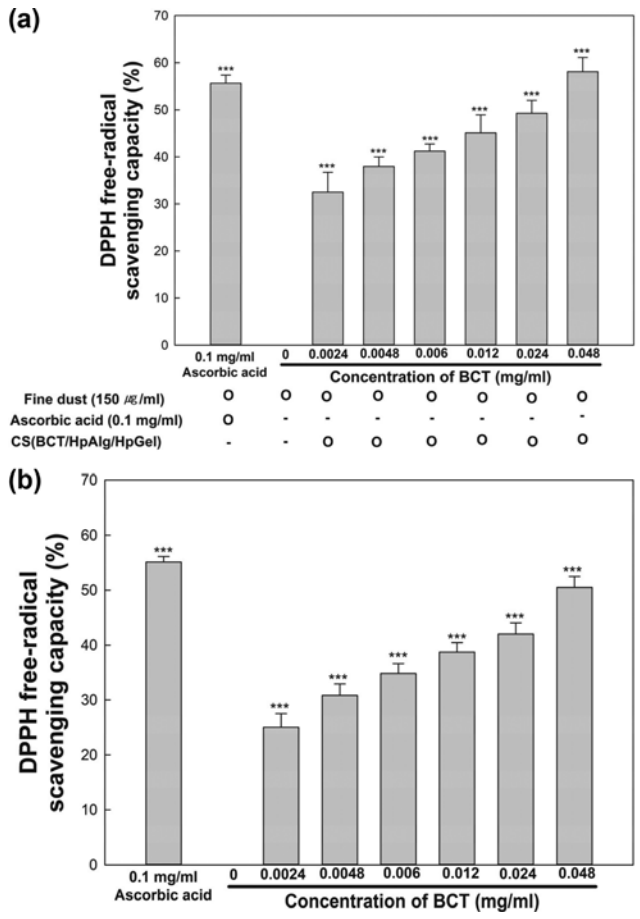

Fig. 4. DPPH radical-scavenging efficacy of CS(BCT/HpAlg/HpGel) (a) and free BCT (b).

5. Intracellular ROS Scavenging Efficacy

The fluorescence intensity of cells untreated with the fine dust was 9815 and that of cells treated with the fine dust was 30985. Thus, it could be said that the carcinogenic fine dust could stimulate RAW 264.7 cell to produce more ROS. Fig. 5(a) shows the ROS SE of CS(BCT/HpAlg/HpGel). Trolox solution (250 μM) exhibited the ROS SE of about 31.7%. Trolox is known to be an antioxidative agent and scavenge ROS effectively [47,48]. CS(BCT/HpAlg/HpGel) exhibited relatively low ROS SE when BCT concentration was 0.012 to 0.24. The ROS SE was about 9.3%, 10.4%, 12.1%, and 14.5%, respectively, when BCT concentration was 0.012, 0.06, 0.12, and 0.24 μg/ml. CS(BCT/HpAlg/HpGel) showed relatively high ROS SE (about 31.7%) when BCT concentration was 0.48 μg/ml. The ROS SE of the CS(BCT/HpAlg/HpGel) suspension (0.48 μg/ml in BCT concentration) was close to that of Trolox solution (250 μM). Fig. 5(b) shows the ROS SE of free BCT solution. No significant ROS SE was observed when BCT concentration was 0.012 and 0.06 μg/ml. ROS SE was about 10.7, 12.9, and 21.4%, respectively, when BCT concentration was 0.12, 0.24, and 0.48 μg/ml. At all the concentrations tested, the ROS SE of BCT loaded in CS(BCT/HpAlg/HpGel) was higher than that of free BCT. The cubosome was thought to have an affinity with cellular membrane because MO, the major component of the cubosome, is amphiphilic and miscible with phospholipid, the major component of the cellular membrane. In addition, RAW 264.7 cell is macrophage-like and it can uptake particulate matters via endocytosis. The affinity with cells and/or the cellular internalization would expedite the transfer of cargo loaded in cubosome to cells, resulting in a higher ROS SE.

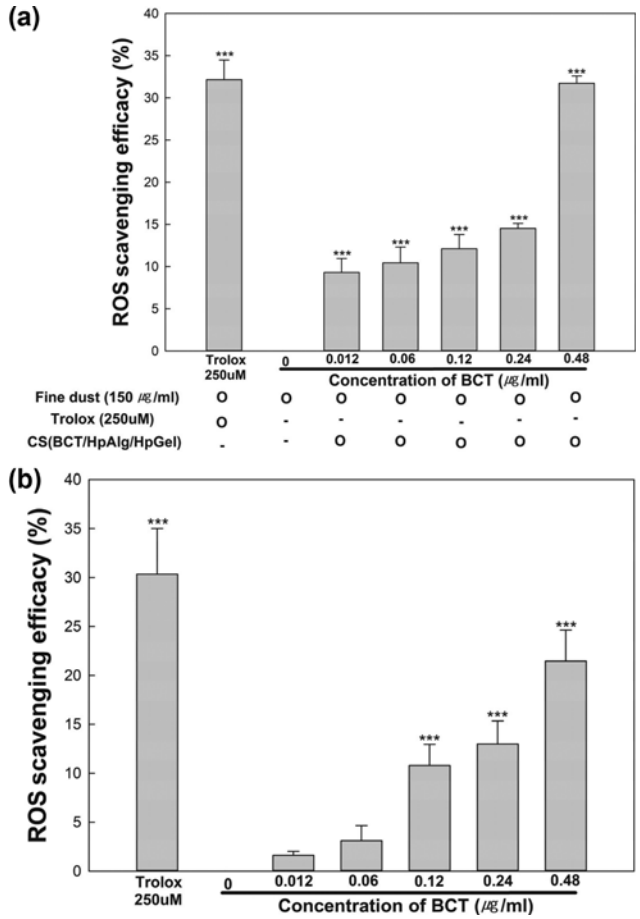

Fig. 5. ROS-scavenging efficacy of CS(BCT/HpAlg/HpGel) (a) and free BCT (b).

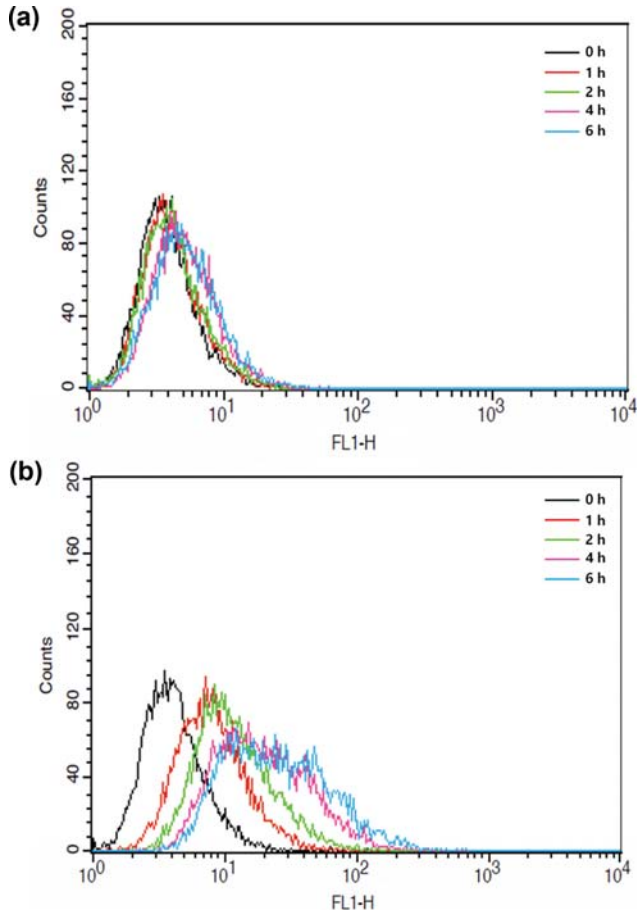

Fig. 6. Flow cytometric profile of Raw 264.7 cells treated with free calcein (a) and cubosomal calcein (calcein loaded in CS(BCT/HpAlg/HpGel)) (b).

6. Cellular Uptake of Cubosomes

Fig. 6(a) shows the flow cytometric profile of Raw 264.7 cells treated with free calcein. As the incubation time increased, the fluorescence geometric mean intensity increased but not markedly. When the incubation period was 0 h, 1 h, 2 h, 4 h, and 6 h, the fluorescence geometric mean intensity was 3.76, 4.06, 4.16, 5.01, and 5.09, respectively. Since calcein is a water-soluble dye, it would hardly be partitioned into the lipidic cellular membrane and internalized into cells. Fig. 6(b) shows the flow cytometric profile of Raw 264.7 cells treated with cubosomal calcein (i.e., calcein loaded in CS(BCT/HpAlg/HpGel)). The fluorescence geometric mean intensity of cells markedly increased with increasing the incubation time. When the incubation period was 0 h, 1 h, 2 h, 4 h, and 6 h, the fluorescence geometric mean intensity was 3.65, 14.49, 18.74, 34.56, and 49.19, respectively. The fluorescence of cells treated with cubosomal calcein was more intensive than that of cells treated with free calcein, suggesting that cubosomal calcein was more bound to and/or internalized into cells than free calcein. It was reported that particulate matters could be taken up by RAW 264.7 cells through phagocytosis [49-52]. The cubosome was thought to be internalized into the cells probably by the endocytosis mechanism, giving a rise to higher fluorescence intensity. Fig. 7(a) shows the SR-CLSM images of Raw 264.7 cell treated with free calcein. The nucleus dyed with DAPI was found as blue circles. Calcein fluorescence was hardly found through the whole period of incubation. As described in FACS, calcein is a water-soluble dye, thus it would hardly be partitioned into the lipidic cellular membrane and transported into the cells. Fig. 7(b) shows the SR-CLSM images of Raw 264.7 cell treated with cubosomal calcein (calcein loaded in CS(BCT/HpAlg/HpGel)). Calcein fluorescein began to appear as light green around nucleus after 1 hr-incubation, and the intensity became stronger as the incubation time increased. This was possibly because the cubosome was internalized into the cells via phagocytosis. Particulate matters are known to be taken up by RAW 264.6 cells via the endocytosis mechanism [53-55]. FACS and SR-CLMS disclosed that the cubosome could facilitate the transfer of its payload (i.e., calcein) to the cells. Thus, the transfer of BCT to the cells would also expedited by the cubosome. This could be a reason why cubosomal BCT was more efficacious than free BCT in scavenging intracellular ROS produced by the cells stimulated by carcinogenic fine dust.

CONCLUSIONS

In vitro anti-oxidative efficacy of BCT loaded in a cubosome (CS(BCT/HpAlg/HpGel) was investigated using carcinogenic fine dust-stimulated RAW 264.7 cells. Polarized optical microscopy revealed that the phase transition temperature of MO cubic phase

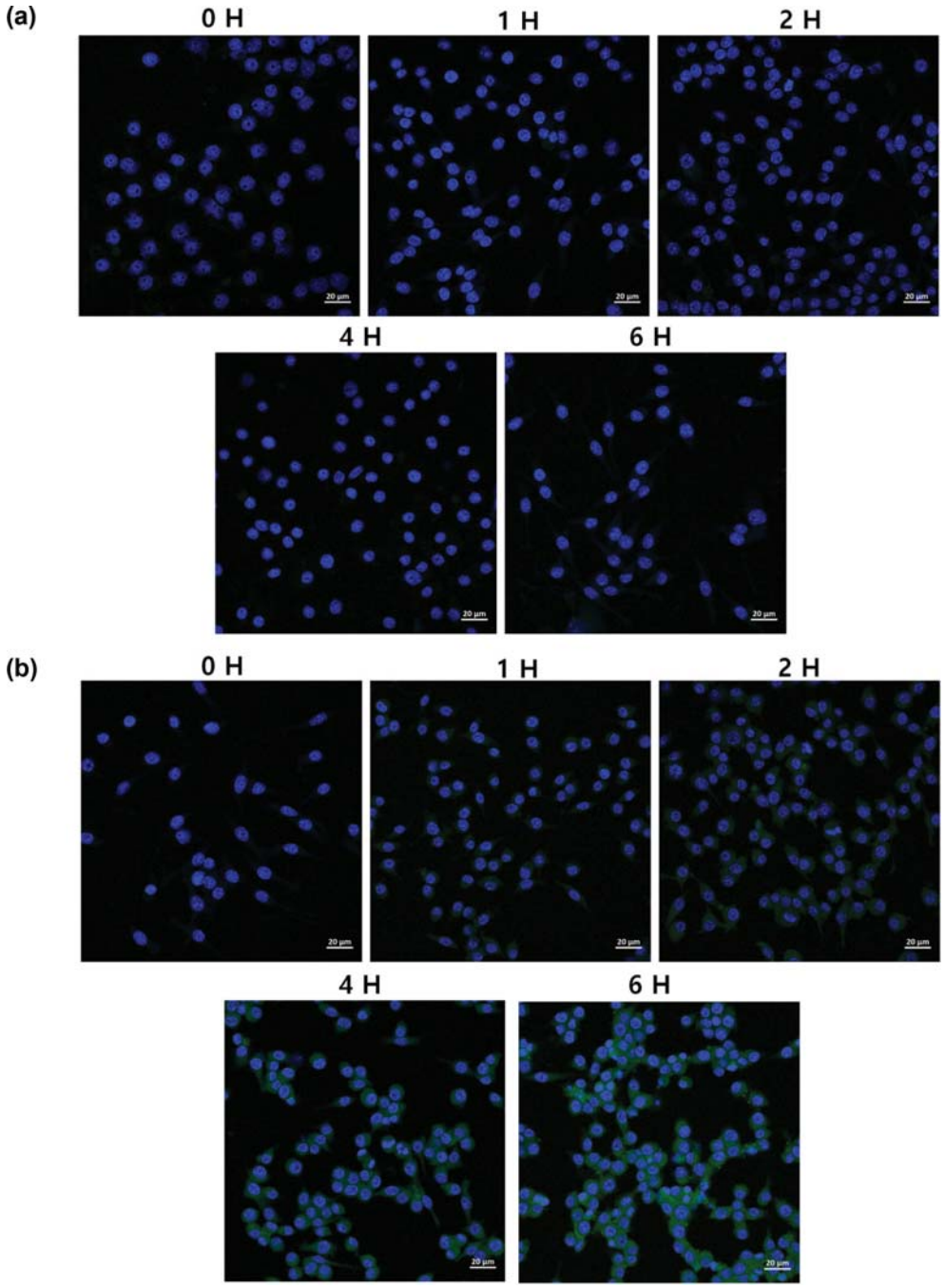

Fig. 7. SR-CLSM images of Raw 264.7 cell treated with free calcein (a) and cubosomal calcein (calcein loaded in CS(BCT/HpAlg/HpGel)) (b).

was lowered by additives (BCT, HpAlg, and HpGel). The size distribution of cubosome was unimodal, the hydrodynamic mean diameter was 148 to 187 nm, and the additive seemed to have little effect on the size. The cubosome markedly enhanced the *in vitro* skin permeation of BCT more than HP-β-CD, a skin permeation enhancer. Cubosomal BCT was more efficacious than free BCT in scavenging DPPH free radical and the intracellular ROS of RAW 264.7 cells stimulated by carcinogenic fine dust. FACS and SR-CLSM disclosed that the cubosome could readily be internalized into the cells, elucidating the reason for the higher radical-scavenging efficacy. Considering the skin permeation-enhancing capability, the cellular internalization property, and the radical scavenging efficacy, the cubosome could be used a carrier for the dermal delivery of BCT to protect skins from oxidative stress caused by carcinogenic fine dust.

ACKNOWLEDGEMENTS

This study was carried out with the support of 'R&D Program for Forest Science Technology (Project No. 2017029D10-1919-BA01)' provided by Korea Forest Service (Korea Forestry Promotion Institute), Basic Science Research Program through the National Research

Foundation of Korea (NRF) funded by the Ministry of Education (No. 2018R1A6A1A03025582).

SUPPORTING INFORMATION

Additional information as noted in the text. This information is available via the Internet at http://www.springer.com/chemistry/journal/11814.

REFERENCES

1. J. C. Shah, Y. Sadhale and D. M. Chilukuri, *Adv. Drug. Deliver. Rev.*, **47**, 229 (2001).
2. C. M. Chang and R. Bodmeier, *Int. J. Pharm.*, **173**, 51 (1998).
3. M. G. Lara, M. V. L. Bentley and J. H. Collett, *Int. J. Pharm.*, **293**, 241 (2005).
4. R. F. Turchiello, F. C. B. Vena, P. H. Maillard, C. S. Souza, M. V. B. L. Bentley and A. C. Tedesco, *J. Photoch. Photobio. B.*, **70**, 1 (2003).
5. C. M. Chang and R. Bodmeier, *Int. J. Pharm.*, **147**, 135 (1997).
6. E. Nazaruk, M. Szlęzak, E. Górecka, R. Bilewicz, Y. M. Osornio, P. Uebelhart and E. M. Landau, *Langmuir*, **30**, 1383 (2014).
7. M. Nakano, T. Teshigawara, A. Sugita, W. Leesajakul, A. Taniguchi, T. Kamo and T. Handa, *Langmuir*, **18**, 9283 (2002).
8. H. Qiu and M. Caffrey, *Biomaterials*, **21**, 223 (2000).
9. C. J. Drummond and C. Fong, *Curr. Opin. Colloid. Interface. Sci.*, **4**, 449 (1999).
10. J. M. Seddon and R. H. Templer, *Phil. Trans. R. Soc. Lond. A.*, **344**, 377 (1993).
11. L. Sagalowicz, M. E. Leser, H. J. Watzke and M. Michel, *Trends. Food Sci. Technol.*, **17**, 204 (2006).
12. S. T. Hyde and S. Andersson, *Z. Kristallogr. Cryst. Mater.*, **168**, 213 (1984).
13. W. Longley and T. J. McIntosh, *Nature*, **303**, 612 (1983).
14. Z. Dong, Y. Ma, K. Hayat, C. Jia, S. Xia and X. Zhang, *J. Food Eng.*, **104**, 455 (2011).
15. T. K. Kwon and J. C. Kim, *Biomacromolecules*, **12**, 466 (2010).
16. M. Bartneck, H. A. Keul, G. Zwadlo-Klarwasser and J. Groll, *Nano. Lett.*, **10**, 59 (2009).
17. N. Oh and J. H. Park, *Int. J. Nanomed.*, **9**, 51 (2014).
18. C. Olbrich, N. Schöler, K. Tabatt, O. Kayser and R. H. Müller, *J. Pharm. Pharmacol.*, **56**, 883 (2004).
19. B. Sarmento, D. Mazzaglia, M. C. Bonferoni, A. P. Neto, M. do Céu Monteiro and V. Seabra, *Carbohyd. Polym.*, **84**, 919 (2011).
20. S. Bancos, D. L. Stevens and K. M. Tyner, *Int. J. Nanomed.*, **10**, 183 (2015).
21. G. Gaucher, K. Asahina, J. Wang and J. C. Leroux, *Biomacromolecules*, **10**, 408 (2009).
22. S. H. Park and J. C. Kim, *Int. J. Polym. Mater. Po.*, Published online (2018).
23. J. Clogston and M. Caffrey, *J. Control. Release.*, **107**, 97 (2005).
24. M. Pisani, S. Bernstorff, C. Ferrero and P. Mariani, *J. Phys. Chem. B.*, **105**, 3109 (2001).
25. M. F. Schulz, F. S. Bates, K. Almdal and K. Mortensen, *Phys. Rev. Lett.*, **73**, 86 (1994).
26. M. Yashima, H. Arashi, M. Kakihana and M. Yoshimura, *J. Am. Ceram. Soc.*, **77**, 1067 (1994).
27. C. J. Howard, B. J. Kennedy and B. C. Chakoumakos, *J. Phys. Condens. Matter*, **12**, 349 (2000).
28. R. G. Matthews, V. I. N. C. E. N. T. Massey and C. C. Sweeley, *J. Biol. Chem.*, **250**, 9294 (1975).
29. P. Kučerová, J. Skopalová, L. Kučera, J. Táborský, H. Švecová, K. Lemr and P. Barták, *Electrochim. Acta*, **215**, 617 (2016).
30. L. M. Cheung, P. C. Cheung and V. E. Ooi, *Food Chem.*, **81**, 249 (2003).
31. C. D. Silva, R. S. Herdeiro, C. J. Mathias, A. D. Panek, C. S. Silveira, V. P. Rodrigues, M. N. Renno, D. Q. Falcao, D. M. Cerqueira, A. B. M. Minto, E. C. A. Eleutherio, C. H. Quaresma, J. F. M. Silva, F. S. Menezes and F. L. P. Nogueira, *Pharmacol. Res.*, **52**, 229 (2005).
32. L. Tian, Y. Zhao, C. Guo and X. Yang, *Carbohyd. Polym.*, **83**, 537 (2011).
33. F. Wang, Y. Han, C. S. Lim, Y. Lu, J. Wang, J. Xu and X. Liu, *Nature*, **463**, 1061 (2010).
34. S. Sridevi and P. V. R. Diwan, *Eur. J. Pharm. Biopharm.*, **54**, 151 (2002).
35. A. Doliwa, S. Santoyo and P. Ygartua, *Drug. Dev. Ind. Pharm.*, **27**, 751 (2001).
36. S. A. Al-Suwayeh, E. I. Taha, F. M. Al-Qahtani, M. O. Ahmed and M. M. Badran, *Sci. World. J.*, **2014**, 9 (2014).
37. Y. Yan, J. Xing, W. Xu, G. Zhao, K. Dong, L. Zhang and K. Wang, *Int. J. Pharm.*, **474**, 182 (2014).
38. K. Wang, Y. Yan, G. Zhao, W. Xu, K. Dong, C. You and J. Xing, *Polym. Chem.*, **5**, 4658 (2014).
39. L. B. Lopes, F. F. Speretta and M. V. L. Bentley, *Eur. J. Pharm. Sci.*, **32**, 209 (2007).
40. L. B. Lopes, D. A. Ferreira, D. de Paula, M. T. J. Garcia, J. A. Thomazini, M. C. Fantini and M. V. L. Bentley, *Pharm. Res.*, **23**, 1332 (2006).
41. H. Herai, T. Gratieri, J. A. Thomazine, M. V. L. B. Bentley and R. F. V. Lopez, *Int. J. Pharm.*, **329**, 88 (2007).
42. T. Rattanapak, K. Young, T. Rades and S. Hook, *J. Pharm. Pharmacol.*, **64**, 1560 (2012).
43. R. Rajan, S. Jose, V. B. Mukund and D. T. Vasudevan, *J. Adv. Pharm. Technol. Res.*, **2**, 138 (2011).
44. R. Re, N. Pellegrini, A. Proteggente, A. Pannala, M. Yang and C. Rice-Evans, *Free Radical Biol. Med.*, **26**, 1231 (1999).
45. D. Zhang and Y. Hamauzu, *Food Chem.*, **88**, 503 (2004).
46. N. J. Miller and C. A. Rice-Evans, *Food Chem.*, **60**, 331 (1997).
47. J. Javanmardi, C. Stushnoff, E. Locke and J. M. Vivanco, *Food Chem.*, **83**, 547 (2003).
48. M. B. Arnao, A. Cano and M. Acosta, *Food Chem.*, **73**, 239 (2001).
49. A. Nishiyama, S. Tsuji, M. Yamashita, R. A. Henriksen, Q. N. Myrvik and Y. Shibata, *Cell. Immunol.*, **239**, 103 (2006).
50. S. Onodera, K. Suzuki, T. Matsuno, K. Kaneda, M. Takagi and J. Nishihira, *Immunology*, **92**, 131 (1997).
51. C. Bianco, F. M. Griffin and S. C. Silverstein, *J. Exp. Med.*, **141**, 1278 (1975).
52. Y. Bi, T. O. Collier, V. M. Goldberg, J. M. Anderson and E. M. Greenfield, *J. Orthop. Res.*, **20**, 696 (2002).
53. Y. Zhang, N. Kohler and M. Zhang, *Biomaterials*, **23**, 1553 (2002).
54. X. Banquy, F. Suarez, A. Argaw, J. M. Rabanel, P. Grutter, J. F. Bouchard and S. Giasson, *Soft Matter*, **5**, 3984 (2009).
55. T. Dos Santos, J. Varela, I. Lynch, A. Salvati and K. A. Dawson, *Small*, **7**, 3341 (2011).